Functional characterization of the RNA interference pathway in *A. fumigatus* reveals its potential for antifungal therapy

Abdulrahman A. Kelani[1], Alexander Bruch[1], Flora Rivieccio[2,3], Corissa Visser[2,3], Thomas Krüger[2,3], Olaf Kniemeyer[2], Michael J. Bromley[4], Paul Bowyer[4], Amelia E. Barber[5], Axel A. Brakhage[2,3], Matthew G. Blango[1]*

[1] Junior Research Group RNA Biology of Fungal Infections, Leibniz Institute for Natural Product Research and Infection Biology—Hans Knöll Institute (Leibniz-HKI), Jena, Germany.

[2] Department of Molecular and Applied Microbiology, Leibniz Institute for Natural Product Research and Infection Biology—Hans Knöll Institute (Leibniz-HKI), Jena, Germany.

[3] Department of Microbiology and Molecular Biology, Institute of Microbiology, Friedrich Schiller University, Jena, Germany.

[4] Manchester Fungal Infection Group, Division of Infection, Immunity and Respiratory Medicine, Faculty of Biology, Medicine and Health, University of Manchester, Manchester, United Kingdom.

[5] Junior Research Group Fungal Informatics, Friedrich Schiller University, Jena, Germany.

Running Title: Leveraging *A. fumigatus* RNAi for therapy

Key Words: RNA interference, filamentous fungi, RNA-based therapeutics

*Correspondence: E-mail matthew.blango@leibniz-hki.de; Tel. +49 (0)3641-532 1072.

ABSTRACT

RNA-based medicines are an emerging class of drugs that are changing the way we treat infectious diseases. The versatility of this class is clearly on display in the rapid design and adaptation of the mRNA vaccines to SARS-CoV-2. Despite the success of these approaches against viruses, research into RNA-based therapeutics to treat human fungal pathogens, a major source of human morbidity and mortality, is lacking. Here, we provide an improved mechanistic description of the RNA interference pathway in *Aspergillus fumigatus* and assess this pathway as a potential target for RNA-based medicines. We describe the genetic variation in RNA interference-associated genes in a large collection of environmental and clinical genomes, reveal the proteins regulated by the RNA interference system using advanced proteomics analysis, and define the components essential for hairpin-induced silencing. We then exploit this pathway using a heterologously expressed hairpin RNA construct to silence the *pabA* gene of *A. fumigatus* to inhibit growth. The data presented here provide a foundation for a mechanistic description of novel RNA regulatory pathways in *A. fumigatus* and reaffirm the importance of improved fungal RNA delivery mechanisms for the future design of RNA-based therapeutics against this important human fungal pathogen.

INTRODUCTION

Human fungal pathogens can cause devastating life-threatening infections that are challenging to diagnose and treat (Fisher et al. 2020). A limited number of therapeutics exist to combat these infections, highlighted in some cases by high cytotoxicity and/or emerging resistance. Previous research efforts have been focused on development of chemical antifungals, immune-based therapies, and vaccine development. Although promising, additional solutions are needed to complement these

approaches and overcome the high clinical burden of human fungal infections. RNA-based therapeutics are only a recent addition to the therapeutic toolkit but have quickly developed into a practical tool in the fight against infectious diseases, like SARS-CoV-2 (Corbett et al. 2020). However, the potential of this new class of therapeutics for treatment of human fungal pathogens remains almost entirely unexplored.

RNA-based therapeutics are being developed to leverage and exploit a variety of different RNA regulatory mechanisms in humans, particularly to correct errors associated with genetic disorders or promote immune responses, as in the case of the mRNA vaccines (Burnett and Rossi 2012; Bruch et al. 2021). In agriculture, the RNA interference (RNAi) pathway of eukaryotic pathogens like fungi and oomycetes has been exploited to silence virulence genes and limit infection using approaches like host-induced gene silencing and spray-induced gene silencing (Cai et al. 2019; Koch et al. 2019). Although in its infancy (Bruch et al. 2021), some intriguing studies have provided hope for RNA-based medicines in treatment of human fungal pathogens, including work defining small molecule inhibitors of fungal group II introns (Fedorova et al. 2018) and development of a 2'-OMethylRNA antisense oligonucleotide against a *Candida albicans* virulence determinant (Araujo et al. 2019).

The most successful strategies in targeting plant fungal pathogens thus far have been centered on the RNAi pathway, which is also frequently leveraged by host organisms to manipulate eukaryotic pathogens (Weiberg et al. 2013; Cai et al. 2018; Hou et al. 2019). RNAi is a conserved molecular mechanism in eukaryotes that was likely intact in the last common ancestor of modern eukaryotes (Shabalina and Koonin 2008). RNAi uses small RNA (sRNA) molecules to suppress gene expression either transcriptionally by heterochromatin recruitment or post-transcriptionally through sequence-specific messenger RNA (mRNA) degradation or translational interference (Moazed 2009; Dang et al.

2011; Torres-Martinez and Ruiz-Vazquez 2017). The first reported example of RNAi in fungi came from the model fungus *Neurospora crassa* as a process termed quelling, where introduction of repetitive transgenes induced post-transcriptional gene silencing (Romano and Macino 1992). Since then, several RNAi and small RNA biogenesis pathways have been characterized in fungi that are largely classified as Dicer-dependent (canonical) RNAi or Dicer-independent (non-canonical) RNAi (Ketting 2011; Ruiz-Vazquez et al. 2015; Torres-Martinez and Ruiz-Vazquez 2017).

Dicer is a type IV RNase III enzyme responsible for dsRNA cleavage and biogenesis of a variety of sRNA classes in different organisms (Nicolas et al. 2015; Torres-Martinez and Ruiz-Vazquez 2017). In fungi, the orthologous RNase III domain-containing enzymes are typically referred to as dicer-like (DCL) proteins due to subtle differences in domain structure. The generated sRNAs are then loaded into an Argonaute protein, the main component of the RNA-induced silencing complex that binds and processes sRNAs to guide selective destruction, translational repression, or transcriptional suppression of target mRNAs (Agrawal et al. 2003; Torres-Martinez and Ruiz-Vazquez 2017). In some instances, RNA-dependent RNA polymerases are required for RNAi pathways to amplify the silencing activity by generating additional dsRNA substrates using the single-stranded sRNAs as primers (Torres-Martinez and Ruiz-Vazquez 2017). While the core RNAi proteins are mostly conserved across eukaryotes, some gene losses and duplications have occurred, which further diversified the RNAi pathways and their functional specialization (Hutvagner and Simard 2008; Mukherjee et al. 2013; Torres-Martinez and Ruiz-Vazquez 2017). Loss of RNAi was observed to fuel hypervirulence in *Cryptococcus* due to higher transposon activity (Gusa et al. 2020), and killer virus-infected *Saccharomyces cerevisiae* strains are able to kill and therefore outcompete non-infected strains in the absence of RNAi (Bostian et al. 1980). The RNAi pathway therefore plays a variety of roles across the fungal kingdom.

In this study, we begin to test the hypothesis that RNA-based therapeutics can be leveraged for treatment of the human fungal pathogen, *Aspergillus fumigatus*, by exploitation of the fungal RNAi pathway. *A. fumigatus* is a ubiquitous, filamentous saprophyte and among the leading fungal killer (Latge 1999; Beauvais et al. 2013). It encodes a functional RNAi system consisting of two dicer-like proteins (DclA and DclB), two argonautes (PpdA and PpdB), and two RNA-dependent RNA Polymerases (RrpA and RrpB), together with several known peripheral factors (**Fig. 1A**) (Mouyna et al. 2004; Hammond and Keller 2005; Hammond et al. 2008b). We find that the RNAi system is highly conserved among clinical strains and environmental isolates of *A. fumigatus*, making it a potential target for therapeutic exploitation. We then define the *A. fumigatus* components required for inverted-repeat transgene silencing and demonstrate that heterologous overexpression of a dsRNA complementary to the *pabA* gene can significantly inhibit growth of the fungus. Collectively, our data suggest that adequate delivery of a properly tailored RNA molecule could hold therapeutic potential in the future.

RESULTS

RNAi pathway genes are conserved in environmental and clinical isolates of *A. fumigatus*.

The development of RNA-based therapeutics against human fungal pathogens will require exploitation of regulatory systems that cannot be easily abandoned by the target organism. To determine whether the RNAi machinery is stably maintained in *A. fumigatus*, we explored the core RNAi components for genetic variation across 300 *A. fumigatus* genomes collected from diverse clinical and environmental niches (Barber et al. 2020; Barber et al. 2021). All the RNAi pathway genes were present as a single copy in the genomes, indicating a high degree of evolutionary conservation. While many strains contained genetic variation, such as missense substitutions or alterations to the 3'UTR (**Fig. S1** and

Dataset S1), high impact variants like frameshifts or premature stops were rare and only observed in 1-6% of samples (n= 4 for *dclA*; n = 1 for *rrpA*; n = 19 for *rrpB*). Of note, the *rrpA* and *rrpB* genes are dispensable for silencing in the related organism *Aspergillus nidulans* (Hammond and Keller 2005), whereas orthologs of the *dclA* gene contribute to the process of meiotic silencing of unpaired DNA during the sexual cycle in other organisms (Alexander et al. 2008). Calculation of the ratio of nonsynonymous to synonymous base changes (d_N/d_S) indicated that all members of the pathway are under purifying selection, often with one paralogous copy of the gene under a stronger degree of selection (**Fig. 1B**). Overall, we find a strong degree of genomic conservation among the *A. fumigatus* RNAi system, which together with the evidence of purifying selection suggests that the pathway likely plays a conserved, beneficial function across *A. fumigatus* strains and that loss does not strongly facilitate virulence in humans as has been hypothesized for other fungal pathogens (D'Souza et al. 2011; Billmyre et al. 2013).

Engineered loss of the RNAi machinery provides no growth advantage in stress or drug challenge.

Genomic analysis suggested that the RNAi machinery is not frequently lost under clinical or environmental conditions, but we wanted to explicitly test the hypothesis that RNAi is dispensable for stress response and drug resistance and ensure that deletion of the machinery is not beneficial to the fungus. To do this, we created a series of knockouts in the core RNAi machinery, including single knockouts of *dclA*, *dclB*, *ppdA*, *ppdB*, *rrpA*, and *rrpB* (**Fig. S2**). In addition, we made a series of pairwise knockouts in *dclA*/B, *ppdA*/*B*, and *rrpA*/*B*. None of the knockouts showed growth defects on minimal or rich media (**Fig. 2A**). Next, we examined the function of RNAi components in response to various stress conditions, including the cell wall stressors congo red, caffeine, and caspofungin; cell membrane stress

agent sodium dodecyl sulfate (SDS); and oxidative stressor H_2O_2. We also tested for sensitivity to azole drugs like voriconazole, tebuconazole, and thiabendazole. In each case, the RNAi knockout strains showed no significant phenotypic difference in comparison to the wild type (**Fig. S3**).

A. fumigatus is a filamentous fungus that reproduces primarily through production of asexual spores called conidia under nutrient limitation (Latge and Chamilos 2019). Conidia are easily aerosolized and after landing in permissive growth conditions can germinate to form hyphae and reinitiate the lifecycle. To determine if the RNAi knockouts might exhibit phenotypes during the asexual lifecycle of *A. fumigatus*, we performed serial passaging of the Δ*dclA/B* and Δ*ppdA/B* double knockouts and a wild-type control strain for 6 generations, as three separate lineages, on AMM agar plates. We omitted the Δ*rrpA/B* strain in this experiment as the RNA-dependent RNA polymerases are thought to be dispensable for silencing based on previous work in the related organism, *Aspergillus nidulans* (Hammond and Keller 2005). Spores were spotted in the center of the plate and allowed to grow at 37°C for 7 days with minimal disturbance to provide numerous rounds of starvation and sporulation. One sublineage of each of the RNAi knockout strains Δ*dclA/B* and Δ*ppdA/B* displayed subtle phenotypes that included white sectoring and altered production of conidia (**Fig. S4**). Previous reports have indicated that these white colonies typically result from mutation of the *pksP* gene, which encodes a polyketide synthase enzyme essential for the initial step in the biosynthesis of dihydroxynaphthalene (DHN) melanin (Langfelder et al. 1998; Gibbons et al. 2022). Conidia collected from the white sectors in our experiment remained white upon transfer to new plates and were confirmed by PCR to hold the appropriate resistance cassette of the knockout. We then counted spore concentrations after a final passaging and observed a small but insignificant decrease in spore

abundance from the Δ*dclA/B* and Δ*ppdA/B* double knockouts (**Fig. 2B**), suggesting that these knockouts may be slightly less reproductive over time.

Proteomics analysis suggests alternative functions for the RNA-dependent RNA polymerases.

The slight decrease in spore abundance over time led us to suspect that the RNAi machinery may play a role as the hyphae begin to run out of nutrients. To take a broader look at hyphae that are preparing for sporulation, we performed LC-MS/MS-based proteomics on 48-hour-old mycelium for each of the double knockout pairs and the wild type. Among the most highly abundant proteins detected at 48 h in the proteomics analysis were an alcohol dehydrogenase (AFUA_7G01010), a Cu/Zn superoxide dismutase (AFUA_5G09240), and several ubiquitin isoforms (AFUA_1G04040 and AFUA_3G11260); results that are consistent with the metabolic changes associated with carbon and iron starvation (Oberegger et al. 2000) (**Dataset S2**). We expected that RNAi-regulated genes would show higher protein abundances in the absence of silencing, and in fact, we did observe several proteins significantly increased in the Δ*dclA/B* and Δ*ppdA/B* strains (**Fig. 3A** and **Fig. S5A-B**). 34 proteins were of higher abundance in Δ*dclA/B* and 44 in the Δ*ppdA/B* strain (**Fig. 3B-C**). Four proteins were found in both strains, namely the hypothetical protein AFUA_4G07200, a putative acyl-CoA dehydrogenase AFUA_1G14850 (cybS), the shikimate pathway enzyme AFUA_1G02110, and a Ran binding domain-containing protein AFUA_6G13260. The Δ*dclA/B* strain had 18 proteins significantly decreased compared to control, whereas the Δ*ppdA/B* strain had 45 proteins lower than wild type. Interestingly, the Δ*rrpA/B* strain had the most differentially detected proteins compared to wild type, despite no obvious link to growth or stress resistance in any of our assays (**Fig. 3D**). 159 proteins were increased in abundance and 56 decreased, with no clear Gene Ontology category enrichment presenting itself to

explain why so many protein levels were altered. When we relaxed the statistical analysis by eliminating the FDR correction, we were able to see some Gene Ontology category enrichment consistent with roles of the RNAi machinery in regulation of RNA regulatory processes (**Fig. S5C-E** and **Dataset S3**).

DclB and PpdA are necessary for hairpin RNA (hpRNA)-mediated gene silencing.

The altered protein landscape of the double knockouts led us to question our understanding of the functionality and redundancy of the individual RNAi components in *A. fumigatus*. To determine which core RNAi factors of *A. fumigatus* are required for silencing of exogenous RNA, we built on a previous study showing that the fungus activates RNAi upon transformation with an inverted-repeat transgene (IRT; (Mouyna et al. 2004)). Sequence complementarity between the inverted-repeat transgene and the *pksP* gene, important for DHN-melanin biosynthesis, led to silencing of *pksP* and an easy phenotypic readout via the production of pigmentless, white conidia (Langfelder et al. 1998).

We reengineered this system using the pSilent-1 gene silencing vector (Nakayashiki et al. 2005) to produce a wild-type strain harboring a Tet-inducible *pksP* inverted-repeat transgene on the *A. fumigatus* chromosome at the *pyrG* locus (**Fig. 4A**). In the wild-type strain, we observed white conidia after induction with doxycycline on AMM plates, indicative of successful post-transcriptional silencing of the *pksP* gene (**Fig. 4B**). Ultimately, we created two versions of these plasmids with different resistance cassettes so that we could also incorporate the construct onto the chromosome in each of our single and double knockouts. While similar silencing was observed in most transformed knockout strains, Δ*dclB* and Δ*ppdA* remained able to produce melanized conidia, suggesting that both DclB and PpdA proteins are essential for hpRNA-dependent silencing and perform functions separate from their

paralogs DclA and PpdB. As mentioned, the RdRPs contribute to the RNA interference pathway in some organisms by transcribing additional dsRNA substrates and amplifying the silencing response (Dang et al. 2011). To eliminate the possibility that the overexpression of our hairpin RNA negated the necessity of the amplification role of RdRPs in *A. fumigatus*, we also passaged the induced RdRP strains onto fresh plates lacking inducer. This experiment allowed us to determine whether the silencing persisted after the induction of the hairpin was removed. In the wild-type, Δ*rrpA*, and Δ*rrpB* strains silencing was quickly lost (**Fig. 4C**), indicating that these proteins likely do not contribute to amplification of silencing in *A. fumigatus* and in agreement with results observed previously in *A. nidulans* (Hammond and Keller 2005). A curious observation is that the loss of silencing occurs to a lower extent than that of wild type, again suggesting a potential alternative function for the RdRP proteins in *A. fumigatus*.

RNAi can potentially be exploited for therapeutic purpose against *A. fumigatus.*

We next tested the potential of exploiting the RNAi machinery using RNA-based therapeutics. Delivery of RNA directly into the fungus has proven to be a challenge previously, as the negatively charged RNA can be sequestered in the cationic cell wall (Jochl et al. 2009). We confirmed this finding in our own system using confocal microscopy to image fluorescein-labelled *in vitro*-transcribed dsRNA accumulation in the cell wall after incubation for 16 hours at 37°C (**Fig. 5A**). The *in vitro*-transcribed dsRNA was created with complementarity to the *A. fumigatus pabA* gene, which encodes a para-aminobenzoic acid synthetase (PabA). PabA catalyzes the biosynthesis of para-aminobenzoic acid (PABA), a precursor for folate biosynthesis in the fungus. Previous work has shown that deletion of *pabA* in *A. fumigatus* and *A. nidulans* results in loss of virulence and severe growth reduction, respectively, lending credence to *pabA* as a potential drug target (Brown et al. 2000). We observed no

cessation of growth in our imaging experiments, consistent with numerous previous studies showing that only minimal silencing can be achieved by the addition of exogenous RNA to *Aspergillus* species (Khatri and Rajam 2007; Abdel-Hadi et al. 2011; Kalleda et al. 2013; Mousavi et al. 2015; Nami et al. 2017). To test if silencing *pabA* would lead to growth repression, we next heterologously expressed a dsRNA hairpin targeting the *pabA* gene from the chromosome of *A. fumigatus*. This heterologous expression experiment was done as before by integrating a 500-bp inverted repeat transgene of *pabA* sequence downstream of an inducible Tet-On promoter. We grew both the *pabA*-IRT-transformed strain and the wild-type strain with and without doxycycline induction on AMM agar plates and liquid cultures. In the absence of doxycycline, the *pabA*-IRT led to minor but significant growth inhibition, likely due to leaky expression (**Fig. 5B**). Upon induction with doxycycline, growth of the *pabA*-IRT-transformed strain was reduced on both AMM agar plates and liquid cultures when compared with the wild-type strain (**Fig. 5B-C**). Growth was more clearly inhibited in liquid culture than on solid media, likely due to more homogenous delivery of the doxycycline inducer. As a control, we also included the *pksP*-IRT strain in our liquid culture experiments and found that this construct also had a growth-inhibiting effect, albeit significantly less than the *pabA*-IRT strain (**Fig. 5B**). As a proof-of-principle, this result provides evidence that *A. fumigatus* growth can be limited by exploiting the RNAi machinery of the organism.

DISCUSSION

Human fungal pathogens remain major global killers and new strategies for treatment are desperately needed. RNA-based therapeutics offer an intriguing conceptual advance, but in practice, remain far away from application against human fungal pathogens in the clinics. Here, we attempted to push the

concept towards our ultimate goal of bringing RNA therapeutics to the clinic by more thoroughly defining the RNAi machinery of *A. fumigatus* and performing a proof-of-principle experiment showing that heterologously expressed RNA can hijack the fungal RNA regulatory machinery to limit growth. Ultimately, we reaffirm that better RNA delivery mechanisms will be required to fully realize the potential of RNA-based therapeutics in fungal pathogens like *A. fumigatus*.

We began by providing a more robust description of the RNAi machinery in *A. fumigatus*. Previous work done in *A. nidulans* laid the groundwork for understanding RNAi in *A. fumigatus*, but distinct differences between the organisms, including truncations of the *A. nidulans* proteins (Hammond and Keller 2005; Hammond et al. 2008a; Hammond et al. 2008b), suggested that additional experimentation could be beneficial. We were able to show that the truncations of some core RNAi components in *A. nidulans* are not commonly repeated in *A. fumigatus*, as 300 sequenced genomes of *A. fumigatus* showed only rare truncation events (e.g. frameshifts) and relatively minor genetic variation. This relatively high level of conservation suggested that we may be able to exploit this machinery for therapeutic purposes, as is being done more frequently with agricultural pests (Cai et al. 2019). Fungal pathogens have been previously observed to lose the RNAi machinery to facilitate virulence (Billmyre et al. 2013; Feretzaki et al. 2016; Nicolas and Garre 2016); however, this does not appear to be the case for *A. fumigatus*. Bolstered by these findings, we were keen to explore the therapeutic potential of exploiting the *A. fumigatus* RNAi machinery. Previous studies in *Aspergillus* species have indicated that there is potential for delivery of RNA into the fungus for silencing (Jochl et al. 2009; Kalleda et al. 2013; Mousavi et al. 2015; Nami et al. 2017), but additional optimization will be required to improve silencing efficiency. New approaches using nanoparticle-based delivery or extracellular vesicles to deliver cargo are on the horizon (Bruch et al. 2021), but finding RNAs that can

inhibit growth remains challenging. Here, we showed that a 500 bp double-stranded RNA with complementarity to the *pabA* mRNA is capable of silencing *pabA* expression to limit fungal growth, but again additional optimization will likely be needed (**Fig. 5**). New approaches using engineered, modified small RNAs offer a unique opportunity that must be investigated further (Bruch et al. 2021). Surprisingly, we also observed that the *pksP*-IRT led to growth inhibition when heterologously expressed. We suspect that the *pksP*-IRT sequence either results in production of small RNAs that have off-target effects or that the overproduction of a double-stranded RNA is mistaken for a mycoviral infection, resulting in altered fungal behavior. Delivery of optimized small RNAs will likely be a more tunable strategy in the long term. It is worth noting that in the literature, heterologous overexpression of a much less structured human mRNA, RBP7, in *A. fumigatus* did not detrimentally alter growth (Shopova et al. 2020) indicating that the phenotype we are observing is not due solely to resource depletion, e.g. nucleotide pool depletion. Ultimately, future studies will be required to fully understand this observation and optimize both delivery and silencing of exogenously delivered RNAs.

To optimize silencing of target genes in *A. fumigatus*, we require a better understanding of the underlying mechanisms of action of the RNAi pathway. As the RNAi machinery has diverse functions in fungi (Lee et al. 2010; Billmyre et al. 2013), we sought to better define the functional components of the RNAi machinery of *A. fumigatus*. Using a previously established inverted-repeat transgene approach (Mouyna et al. 2004), we created an inducible hairpin RNA against the *pksP* gene of *A. fumigatus*, which is required for production of DHN-melanin and the grey-green color of conidia. With this approach, we were able to determine that DclB and PpdA are required for inverted-repeat transgene silencing in *A. fumigatus*, whereas the other core components are dispensable for this form of RNA silencing. The finding that DclB and PpdA are essential for silencing matches previous work in *N.*

crassa, where DCL-2 and QDE-2, orthologs of DclB and PpdA, were shown to be important for quelling (Dang et al. 2011). Unlike *N. crassa*, DclA was not able to compensate in a Δ*dclB* deletion strain of *A. fumigatus* in our *pksP*-inverted-repeat transgene silencing experiments, suggesting discrete functions for DclA, perhaps during the poorly understood *A. fumigatus* sexual cycle.

The RNAi pathway in fungi has been linked to diverse regulation, including in sexual differentiation, development, stress response, and growth (Ruiz-Vazquez et al. 2015; Nicolas and Garre 2016; Torres-Martinez and Ruiz-Vazquez 2017). Despite all these important functions in other organisms, *A. fumigatus* appears to be more robust in tolerating deletion of the core RNAi machinery, which is somewhat paradoxical based on the results of our genomics analysis. Minimal functional differences were observed in a wide array of stress assays, suggesting that novel features of RNAi may be identifiable in *A. fumigatus*. RNAi pathways also frequently play an important role in maintaining genome integrity, as has been described in distantly related fungal pathogens *Cryptococcus neoformans* (Janbon et al. 2010; Wang et al. 2012), *Mucor circinelloides* (Nicolas et al. 2010; Calo et al. 2017), *Fusarium graminearum* (Chen et al. 2015), *Magnaporthe oryzae* (Kadotani et al. 2003; Murata et al. 2007), and *Trichoderma atroviride* (Carreras-Villasenor et al. 2013). Investigation of fungal RNAi has proven a function in preserving the integrity of the host genome against invasive nucleic acids including transgenes, transposons, and invading viruses during both the vegetative and sexual cycles (Nuss 2011; Torres-Martinez and Ruiz-Vazquez 2017). The *A. fumigatus* Af293 strain is known to be infected with a mycovirus that can modify fungal growth and virulence (Kanhayuwa et al. 2015) and trigger small RNA production (Ozkan et al. 2017). It will be interesting to see if the RNAi machinery is intact and active in this strain where a mycovirus has overcome fungal defenses. Future studies into

the RNAi components that contribute to genome protection are now possible using the tools we created here.

Taken together, the results presented here improve our understanding of the RNAi pathway in an important human pathogen and lay a foundation for the development of RNA-based therapeutics against *A. fumigatus*. The more mechanistic understanding of *A. fumigatus* RNA silencing provided here will serve as a tool in the design of more intelligent RNA therapeutics and enable additional work into the RNA silencing mechanism of this pathogen. Coupled with the explosion of research into extracellular vesicles and nanoparticles as RNA delivery devices (Brakhage et al. 2021; Witwer and Wolfram 2021), together with improvements in design of RNA medicines against other human maladies, we anticipate a future where RNA will play a key role in the fight against human fungal pathogens.

MATERIALS AND METHODS

Domain mapping and genomic analysis.

Domain structures were created using UniProt annotations (Uniprot.org; Q4WSH7, Q4WY64, Q4WEW6, Q4WWR4, Q4WUR8, Q4WC92, Q4WXX3, Q4WA22, and Q4WVE3) and created with the drawProteins (Brennan 2018) package using R version 4.1.0 (2021-05-18).

The genomic data analyzed in this study was generated in (Barber et al. 2021) and is publicly available as raw reads and assembled genomes under PRJNA697844 and PRJNA595552. Isolates originated from environmental and clinical sources and displayed a global distribution. Presence/absence variation in the genomes was quantified using Orthofinder using peptide sequences from 300 genomes. Given that no cases of gene loss or amplification were detected among the

genome assemblies, analysis of sequence variation was performed by aligning raw sequencing reads to the Af293 reference genome (FungiDB release 39). PCR duplicates were marked using MarkDuplicate from Picard v.2.18.25. Variant calling to detect SNVs and short indels was performed using HaplotypeCaller and high-quality variants identified using the following filtering criteria: SNP: QD < 2.0 || MQ < 40.0 || FS > 60.0 || MQ RankSum < −12.5 || ReadPosRankSum < −8.0; indel: QD < 2.0 || FS > 200.0 || ReadPosRankSum < −20.0. Variant function was predicted using SnpEff v.4.3.

Strains and culture conditions.

A. fumigatus strains were grown on *Aspergillus* minimal medium (AMM) agar plates (70 mM $NaNO_3$, 11.2 mM KH_2PO_4, 7 mM KCl, 2 mM $MgSO_4$, 1% (w/v) glucose and 1 µl/ml trace element solution (pH 6.5)). The trace element solution was composed of 1 g $FeSO_4 \bullet 7\ H_2O$, 8.8 g $ZnSO_4 \bullet 7\ H_2O$, 0.4 g $CuSO_4 \bullet 5\ H_2O$, 0.15 g $MnSO_4 \bullet H_2O$, 0.1 g $NaB_4O_7 \bullet 10\ H_2O$, 0.05 g $(NH_4)_6Mo_7O_{24} \bullet 4\ H_2O$, and ultra-filtrated water to 1000 ml. Spores were harvested after 5 days (or 7 days for the evolution experiment) with 10 ml of sterile distilled water using a T-shaped inoculation spreader and spore suspensions were filtered through a 30-µm cell strainer (MACS, Miltenyi Biotec GmbH, Germany) to exclude mycelia. *A. fumigatus* transformants were screened on AMM agar plates supplemented with 150 µg/ml of hygromycin, 0.1 µg/ml of pyrithiamine, or 160 µg/ml of phleomycin for selection. For *in vitro* transcription and confocal laser scanning microscopy experiments, *A. fumigatus* AfS150 was grown on malt agar (Sigma-Aldrich) plates supplemented with agar to a final concentration of 2% (wt/vol) for 5 days. *Escherichia coli* strains were grown at 37°C on LB broth or agar supplemented with 100 µg/ml carbenicillin when necessary.

Genetic manipulation strategies.

Knockout constructs were created using several strategies, namely Fusion PCR or the Gibson cloning method (9). To make constructs by Fusion PCR (10), an antibiotic selection gene and approximately 1 kb of DNA flanking regions (5´ and 3´) of the target gene were amplified. PCR fragments were purified using the GeneJET PCR Purification Kit (Thermo Fisher Scientific; Vilnius, Lithuania) and concentrations were measured by NanoDrop 2000 spectrophotometer. Next, equimolar amounts of the three fragments, two flanking regions, and selection gene, were combined using Fusion PCR with the 2x Phusion Flash High Fidelity Master Mix and 10 pmol of each forward and reverse primer for the 5´ flank and 3´ flank, respectively. Fusion PCR products were purified and validated by agarose gel electrophoresis. For Gibson assembly, a selection gene and about 1 kb flanking regions of target gene were amplified by PCR using primers that create overhangs (**Table S1**). In addition, pUC18 vector backbone was also amplified from plasmid "pUChph Volker". DNA fragments were assembled and the resulting plasmid was used to transform chemically-competent *E. coli* following the NEBuilder HiFi DNA Assembly protocol (New England Biolabs; Ipswich, United States). Knockouts of *A. fumigatus* were generated by homologous recombination following the transformation of protoplasts (Weidner et al. 1998).

Growth and viability assays.

The growth capacity of different *A. fumigatus* strains in AMM media was investigated by determining the dry weight from shaking cultures. $1x10^7$ spores were inoculated in 50 ml AMM and incubated at 37°C and 200 rpm for 24 hours. Mycelia were harvested using Miracloth (Merck KGaA; Darmstadt, Germany), washed with deionized water, and dried at 60°C for 3 days. The susceptibility of different *A.*

fumigatus strains to stress conditions was investigated by spotting 5 µl of spore suspension with concentrations ranging from 10^5-10^2/ml on AMM agar plates supplemented with different stress-inducing agents for 2 days. All plates were incubated at 37°C.

Inverted-repeat transgene (IRT) silencing assays.

To silence *A. fumigatus pksP*, sense and anti-sense *pksP* PCR product (500 bp each) were amplified with primer pairs oARK 0031 & 0032 and oARK 0033 & 0034 respectively. These PCR products were then cloned into the two multi-cloning sites in the p-Silent1 plasmid vector, which already has a hygromycin resistant cassette. The *trpC* promoter upstream the inverted-repeat region original present from the p-Silent 1 vector was replaced by a tetracycline inducible promoter (TetON). The resulting plasmid was then digested with restriction enzymes *SacI* and *FspI* to excise the IRT expressing region and hygromycin (hph) resistant cassette, which was then cloned into a pUC18 vector backbone flanked by 5′ and 3′ regions (approximately 1 kb) of a non-functional *pyrG* locus in the CEA17Δ*akuB*^{KU80} (A1163) strain to generate pSilent-pksP1. Because some of the RNAi knockout strains already have a hygromycin resistant cassette, we constructed pSilent-pksP2 by replacing the selection marker with a phleomycin (ble) resistant gene. Both plasmids were linearized by *BtsI* restriction enzyme before transformation of strains (**Table S2**). To generate a para-aminobenzoic acid synthetase (*pabA*) silencing construct, pabA-IRT sequence plus a 3' *trpC* terminator was synthesized. This synthesized DNA was then cloned using Gibson assembly into a PCR product amplified from pSilent-pksP2 with primer pair oARK0096 & oARK0038. The latter PCR product consist of the pUC18 backbone, *pyrG* flanks, phleomycin resistant cassette, and TetON promoter to drive the pabA-IRT expression. Plasmid was linearized by *PstI* restriction enzyme before transformation of CEA17Δ*akuB*^{KU80} wild-type strain.

Southern blot.

Target gene deletion was confirmed by Southern blot, as described previously (Southern 2006). Digested genomic DNA samples were separated in a 1% (w/v) agarose gel. Separated DNA fragments on gel were transferred onto a nylon membrane (pore size: 0.45 µm, Carl Roth GmbH; Karlsruhe, Germany). The DNA was crosslinked to the membrane by UV irradiation followed by overnight hybridization with a DIG-11-dUTP-labelled DNA probe at 65°C. The membrane was washed twice at 65°C for 5 minutes (1x SSC, 0.1 SDS), followed by 2 washes with wash buffer II (0.5x SSC, 0.1 SDS) for 20 minutes at 65°C. The membrane was next rinsed with maleic acid wash buffer, incubated with blocking solution for 30 minutes to prevent unspecific antibody binding, followed by another incubation with 20 ml blocking solution plus 0.5 µl Anti-Digoxigenin-AP, Fab fragments (Roche, Mannheim, Germany) for 30 minutes. The unbound antibodies were removed by washing twice with 50 ml maleic acid wash buffer for 15 minutes. Finally, the membrane was equilibrated with detection buffer, developed with several drops of the chemiluminescent substrate CDP-Star, ready-to-use (Roche) and detected with a Chemiluminescence Imaging – Fusion FX SPECTRA instrument (Vilber Lourmat, Collégien France).

***In vitro* transcription and confocal laser scanning microscopy.**

For *in vitro* dsRNA transcription, genomic DNA was isolated from mycelium of *A. fumigatus* CEA17Δ*akuB* grown overnight in liquid cultures and used as template for the amplification of 500 base pairs of the *pabA* sequence by PCR. The PCR reaction mix consisted of 200-300 ng template DNA, 10 pmol of each primer and 25 µl of 2x Phusion Flash High-Fidelity PCR Master Mix (Thermo Fisher Scientific). Both, the forward and the reverse primer were designed to contain a T7 promotor at their

5' end for subsequent dsRNA transcription (**Table S1**; T7_pabA_500_1_for/T7_pab_A500_1_rev). PCR products were loaded onto a 1% agarose gel to check for the correct size and purified with the GeneJET PCR Purification kit (Thermo Fisher Scientific). The products were then used as template for *in vitro* dsRNA transcription using the MEGAscript RNAi Kit (Invitrogen) according to the manufacturer's protocol with slight modifications. Briefly, the transcription reaction was assembled as specified with the addition of 0.5 µl fluorescein-labelled-UTP Solution (Sigma-Aldrich). The reaction was incubated at 37°C for 4 h and the RNA products were annealed by heating the reaction to 75°C for 5 min and subsequently left to cool at room temperature. Digestion of DNA and single-stranded RNA and the purification of dsRNA was performed as described in the protocol with the exception that the purified dsRNA was eluted in two steps using a total of 100 µL of 95°C ultrapure H_2O. Quantity and quality of the dsRNA was assessed by fluorometric analysis using a Qubit 4 Fluorometer (Thermo Fisher Scientific). dsRNA was stored in the dark at -80°C until usage.

For fluorescence microscopy, $1x10^4$ freshly collected *A. fumigatus* AfS150 conidia (Lother et al. 2014) were seeded into each well of a 8-well chamber slide (µ-Slide 8 Well, Ibidi) in a total of 100 µl RPMI medium (Sigma-Aldrich), treated with 2 µg of labelled dsRNA, and incubated at 37°C and 5% CO_2 (v/v) for 16 h. The following day, old media was removed from the samples and fresh media containing calcofluor white was added to the fungus. After 30 minutes of incubation at room temperature in the dark, hyphae were carefully washed with sterile phosphate-buffered saline (PBS). 100 µl RPMI was added to each chamber and samples were observed by confocal laser scanning microscopy with a Zeiss LSM 780 microscope (Carl Zeiss). Images were processed using the ZEN blue edition software (version 3.4, Carl Zeiss).

Proteome analysis

Harvested cells were disrupted by mortar and pestle with liquid nitrogen. Cell debris were homogenized in lysis buffer (1% (w/v) SDS, 150 mM NaCl, 100 mM TEAB (triethyl ammonium bicarbonate), one tablet of cOmplete Ultra Protease Inhibitor Cocktail). After addition of 0.5 µl Benzonase nuclease (250 U/µl) the samples were incubated at 37°C in a water bath sonicator for 30 min. Proteins were separated from insolubilized debris by centrifugation (15 min, 18000 × g). Each 100 µg of total protein per sample was diluted with 100 mM TEAB to gain a final volume of 100 µl. Subsequently, cysteine thiols were reduced and carbamidomethylated for 30 min at 70°C by addition of each 2 µl of 500 mM TCEP (tris(2-carboxyethyl)phosphine) and 625 mM 2-chloroacetamide (CAA). The samples were further cleaned up by methanol-chloroform-water precipitation using the protocol of Wessel and Flügge (Wessel and Flugge 1984). Protein precipitates were resolubilized in 5% trifluoroethanol of aqueous 100 mM TEAB and digested for 18 h with Trypsin+LysC (Promega) at a ratio of 25:1 protein:protease. Samples were evaporated in a vacuum concentrator (Eppendorf). Tryptic peptides were resolubilized in 30 µl of 0.05% TFA and 2% ACN in H_2O filtered through 10 kDa MWCO PES membrane spin filters (VWR) at 14,000×*g* for 15 min and transferred to HPLC vials.

LC-MS/MS analysis was performed on an Ultimate 3000 RSLCnano system connected to a QExactive Plus mass spectrometer (Thermo Fisher Scientific, Waltham, MA, USA). Peptide trapping for 5 min on an Acclaim Pep Map 100 column (2 cm × 75 µm, 3 µm) at 5 µl/min was followed by separation on an analytical Acclaim Pep Map RSLC nano column (50 cm × 75 µm, 2 µm). Mobile phase gradient elution of eluent A (0.1% (v/v) formic acid in water) mixed with eluent B (0.1% (v/v) formic acid in 90/10 acetonitrile/water) was performed using the following gradient: 0–5 min at 4% B, 30 min at 7%

B, 60 min at 10% B, 100 min at 15% B, 140 min at 25% B, 180 min at 45% B, 200 min at 65%, 210–215 min at 96% B, 215.1–240 min at 4% B.

Positively charged ions were generated at a spray voltage of 2.2 kV using a stainless-steel emitter attached to the Nanospray Flex Ion Source (Thermo Fisher Scientific). The mass spectrometry instrument was operated in data dependent MS2 Top15 mode. Precursor ions were monitored at m/z 300-1500 at a resolution of 140,000 FWHM (full width at half maximum) using a maximum injection time (ITmax) of 120 ms and an AGC (automatic gain control) target of 3×10^6. Precursor ions with a charge state of z=2–5 were isolated at a width of m/z 1.6 amu for HCD fragmentation at 30% normalized collision energy. MS2 ions were scanned at 17,500 FWHM (ITmax=120 ms, AGC= 2×10^5). Dynamic exclusion of precursor ions was set to 30 s.

Tandem mass spectra were searched against the FungiDB database (https://fungidb.org/common/downloads/Current_Release/AfumigatusAf293/fasta/data/FungiDB-57_AfumigatusAf293_AnnotatedProteins.fasta) of *Aspergillus fumigatus* Af293 (2021/07/09; YYYY/MM/DD) using Proteome Discoverer (PD) 2.4 (Thermo) and the algorithms of Mascot 2.4.1 (Matrix Science, UK), Sequest HT (version of PD2.4), MS Amanda 2.0, and MS Fragger 3.2. Two missed cleavages were allowed for the tryptic digestion. The precursor mass tolerance was set to 10 ppm and the fragment mass tolerance was set to 0.02 Da. Modifications were defined as dynamic Met oxidation, protein N-term Met-loss and/or acetylation as well as static Cys carbamidomethylation. A strict false discovery rate (FDR) < 1% (peptide and protein level) and a search engine score of > 30 (Mascot), > 4 (Sequest HT), > 300 (MS Amanda) or > 8 (MS Fragger) was required for positive protein hits. The Percolator node of PD2.4 and a reverse decoy database was used for q value validation of spectral matches. Only rank 1 proteins and peptides of the top scored proteins were counted. Label-

free protein quantification was based on the Minora algorithm of PD2.4 using the precursor abundance based on intensity and a signal-to-noise ratio > 5. Normalization was performed by using the total peptide amount method. Imputation of missing quan values was applied by using abundance values of 75% of the lowest abundance identified per sample. Differential protein abundance was defined as a fold change of > 2, ratio-adjusted p-value <0.05 (p-value/log4ratio) and at least identified in 2 of 3 replicates of the sample group with the highest abundance.

Data availability

The mass spectrometry proteomics data were deposited in the ProteomeXchange Consortium via the PRIDE partner repository (Perez-Riverol et al. 2022) with the dataset identifier PXD033984.

Statistical Analysis. The proteomics data were analyzed as described. For the remaining analyses, P values were determined by ANOVA or two-tailed Student's t-tests where appropriate using Prism 5.0.0 software (GraphPad Software). Differences between the groups were considered significant at a P value of <0.05. Throughout the article, significance is denoted as follows: *, P = <0.05; **, P = <0.01, ***, P = <0.001; ns, nonsignificant.

ACKNOWLEDGEMENTS

We would like to thank Pamela Lehenberger, Carmen Schult, and Laura Broschat for excellent technical assistance. The work presented here was generously supported by the Federal Ministry for Education and Research (BMBF: https://www.bmbf.de/), Germany, Project FKZ 01K12012 "RFIN – RNA-Biologie von Pilzinfektionen" and the Deutsche Forschungsgemeinschaft (DFG)-funded Collaborative Research

Center/Transregio FungiNet 124 'Pathogenic fungi and their human host: Networks of Interaction' (210879364, project A1 and Z2). The authors declare no conflicts of interest.

FIGURE LEGENDS

FIG 1. RNAi is conserved across 300 sequenced *A. fumigatus* strains.

(A) Structural domains of *A. fumigatus* RNAi proteins were analyzed using UniProt (www.uniprot.org/). DclA and DclB both contain a DExH-helicase followed by a helicase-C, a Dicer- dsRNA binding fold that mediates binding with other proteins (Qin et al. 2010), a P-element-induced wimpy testis (PIWI)–Argonaute–Zwille (PAZ) domain for binding the 3' end of the dsRNA, and two RNase III domains necessary for cleavage of bound dsRNA (Schauer et al. 2002; Mukherjee et al. 2013; Song and Rossi 2017). Both argonaute orthologs (PpdA/B) have the characteristic PAZ domain and a PIWI domain present in all eukaryotic argonautes (Jinek and Doudna 2009; Ender and Meister 2010). **(B)** Calculation of dN/dS ratios for each of the core RNAi components and peripheral factors using 300 genomes from (Barber et al. 2021). Ratios under 1 indicate that each gene is under neutral-to-purifying selection.

FIG 2. Deletion of RNAi components does not affect fitness.

(A) Droplet growth assays for wild-type (WT), *ΔdclA/B*, *ΔppdA/B*, and *ΔrrpA/B* strains grown on AMM or Malt agar plates for 48 hours. Image shown is representative of three independent experiments. **(B)** Double knockout strains were grown as 3 biological lineages and passaged for 6 generations on AMM agar plates at 37°C for 7 days. The evolved strains were then grown for an additional week and the spores were counted using a CASY counter. The plot shows the means of the values from the three lineages +/- standard deviation.

FIG 3. Proteomics reveals altered protein abundance in double knockouts.

(A) Clustered heatmap depicting expression ratios for double knockouts relative to wild type for cases where proteins exhibited at least 4-fold change and a *p*-value < 0.01 in one of the conditions. **(B-D)** Volcano plots showing expression ratio for double knockout compared to wild type for **(B)** Δ*dclA/B*, **(C)** Δ*ppdA/B*, and **(D)** Δ*rrpA/B*. The y-axis shows the -$\log_{10}$ transformed *p*-value, where higher values are more significant. Orange circles show proteins that are at least 2-fold changed and with a *p*-value less than 0.05.

FIG 4. DclB and PpdA are required for IRT-mediated silencing in *A. fumigatus*.

(A) Schematic diagram of the constructs (pSilent-*pksP*1 and pSilent-*pksP*2) used to induce RNAi. Sense and anti-sense *pksP* PCR product (**green**) were placed downstream of an inducible Tet-On promoter (**blue**). The inverted-repeat region and antifungal selection genes (***hph*** and ***ble***) for each plasmid were collectively flanked by 5′ and 3′ regions (**black**) amplified from template of a non-functional *pyrG* locus for homologous recombination. **(B)** Wild-type and RNAi knockout strains transformed with IRT constructs were spot inoculated on AMM with and without inducer (10 µg/ml doxycycline, **dox**) for 2 days. Image shown is representative of three independent experiments. **(C)** Wild-type and IRT-transformed strains were spot inoculated on AMM agar plates without inducer (10 µg/ml doxycycline) for 2 days. Spores were collected and the experiment was repeated without IRT induction.

FIG 5. The RNAi pathway can be exploited to limit fungal growth.

(A) The *A. fumigatus* cell wall limits the delivery of extracellular RNA as shown by confocal laser scanning microscopy of calcofluor white-stained (blue) *A. fumigatus* AfS150 hyphae expressing a cytoplasmic dTomato (red), which were incubated with *in vitro*-transcribed fluorescein-UTP labelled dsRNA (green). **(B)** The wild-type (CEA17Δ*akuB*^{KU80}) strain was transformed with a plasmid (pSilent-*pabA*) expressing a dox-inducible IRT targeting *pabA*, a para-aminobenzoic acid synthetase-encoding gene. Wild-type and *pabA*-IRT expressing strains, as well as a control *pksP*-IRT expressing strain were grown with and without dox induction for 24. Mycelia were collected and dried at 60°C for 3 days before measuring weight. **(C)** Wild-type and *pabA*-IRT expressing strain were spot inoculated on AMM agar plates supplemented with different concentrations of dox. Images were taken after 2 days of incubation at 37°C. Plot displays data from 4 biological replicates, with each replicate having 3 technical repeats. Significance was determined by t test with Bonferroni correction following 2-way ANOVA.

SUPPLEMENTARY FIGURES

FIG S1. The RNAi machinery incurs only minor-to-moderate genetic variation.

Histogram depicting the number of variants and their functional impact in RNAi genes from 300 of *A. fumigatus* genomes. Genetic changes are reported relative to the Af293 reference genome. DNA base changes resulting in synonymous substitutions or those in intergenic regions are not shown. Full summary in **Dataset S1**.

FIG S2. Southern blot validation of knockout strains.

(A) Southern blot images showing confirmation of gene deletions in knockout strains. Numbers indicate candidate knockout strains collected from transformation plates. Candidates were digested with appropriate restriction enzymes to produce fragments of differing sizes in the wild type and knockout for each gene. One of the flanking regions was used as the probe by using primers from the creation of the knockout as well as the addition of DIG-UTP to the PCR reaction. Stars indicate strains with construct of anticipated size.

FIG S3. RNAi does not contribute to stress response or drug resistance.

(A) Droplet stress assays for wild-type (WT), *ΔdclA/B*, *ΔppdA/B*, and *ΔrrpA/B* strains grown on AMM agar plates supplemented with indicated stress inducers. Images shown for each stress condition are representative of three independent experiment after 48 hours. Wild-type and RNAi double knockouts were grown on increasing concentrations of (**B**) voriconazole and (**C**) tebuconazole. The MIC was determined after 48 hours.

FIG S4. Images of fungal strains evolved over six generations without selective pressure.

Double knockout strains were grown as 3 biological lineages and passaged for 6 generations on AMM agar plates. Each generation was allowed to grow at 37°C for 7 days before the next passage. Each plate for each lineage was photographed before harvesting spores. The slight color changes are due to changes in ambient light during image acquisition.

FIG S5. Proteome analysis of combined RNAi mutants.

Overlapping **(A)** upregulated or **(B)** downregulated proteins of the indicated set of strains are displayed by Venn diagrams (created with http://bioinformatics.psb.ugent.be/webtools/Venn/). **(C-E)** The proteins with altered abundances from each individual mutant were subjected to Gene Ontology (GO) analysis (Ashburner et al. 2000; Gene Ontology 2021). The top three GO categories of the increased (yellow bars) or decreased (blue bars) proteins are listed for every strain.

SUPPLEMENTARY TABLES

Table S1. Oligonucleotides used in this study.

Oligonucleotide	Sequence (5`- 3`)	Target gene
dclA_P1_for	CGTGTAGCTTCTTCTCATTG	Afu5g11790
dclA_ ptrA _P2_rev	GGCCTGAGTGGCCATCGAATTCGAATGGCTGGGTTGGAAAGG	Afu5g11790
dclA_ptrA_P3_for	GAGGCCATCTAGGCCATCAAGCCTCTGGAGGTATGGACGAAG	Afu5g11790
dclA_P4_rev	GACAGAGGCGACCGTAGTAG	Afu5g11790
dclB_P1_for	AGCAAGAACAAACGCATGGC	Afu4g02930
dclB_hph_P2_rev	CTGCAGATATCCATCACACTGGCGAGGAAAGTCCTCATTCTCCC	Afu4g02930
dclB_hph_P3_for	GAAGGGCGAATTCCAGCACACTGAGTACTTCCGAGATTTCGCG	Afu4g02930
dclB_P4_rev	TAACTCGACTCAACAGCTGC	Afu4g02930
ppdA_pUC18_P1_for	GTCGACTCTAGAGGATCCCCGGAACTTGATTTGTCGGTCG	Afu8g05280
ppdA_ble_P2_rev	GGCCTTTCCGGTTTCATACACCGGGCAAAGAGGAAGATTGGGTTAAGCGC	Afu8g05280
ppdA_ble_P3_for	CGTTTACCCAGAATGCACAGGTACACTTGTCGAATGGACTTTCCAACTGC	Afu8g05280
ppdA_pUC18_P4_rev	GAATTCGAGCTCGGTACCAAACGCATTTCGACCTCACG	Afu8g05280
ppdB_P1_for	CGCAATAGCCGACCTGCATC	Afu3g11010
ppdB_ptrA_P2_rev	GGCCTGAGTGGCCATCGAATTCGCGGGCGAGATAGTGCAGTG	Afu3g11010
ppdB_ptrA_P3_for	GAGGCCATCTAGGCCATCAAGCCTGCCCATTCATGGTACCTC	Afu3g11010
ppdB_P4_rev	CACTGCTGTTGCTTCCCTTG	Afu3g11010
rrpA_P1_for	TCGTACATGCTTGTTCCAGC	Afu3g06790
rrpA_ptrA_P2_rev	GGCCTGAGTGGCCATCGAATTCGAAGATGGGTAAGAGGAAGG	Afu3g06790
rrpA_ptrA_P3_for	GAGGCCATCTAGGCCATCAAGCGTTCTAGTCGGCTTTCTAGG	Afu3g06790
rrpA_P4_rev	ATTGAAGGAGCAGCATCTGC	Afu3g06790
rrpB_P1_for	TTACCCAGCAACAGTAACGG	Afu5g09430
rrpB_hph_P2_rev	CTGCAGATATCCATCACACTGGCGCTCAGCTAAGGAATCCATCC	Afu5g09430
rrpB_hph_P3_for	GAAGGGCGAATTCCAGCACACTGCGGAACTCTCTTAGGTATGG	Afu5g09430

rrpB_P4_rev	ACACCCCTAATAGTTAAAATGGG	Afu5g09430
coxV_for	ATCTGTTCGCCAAGCCCAAG	Afu5g10560
coxV_rev	TCACTGCTGACACCGTAGAG	Afu5g10560
oARK0027_for	ACCTCGAGGTACGTACAAGCTTAAACCTCCTTACTAACCCGG	Afu2g17600 (*pksP*)
oARK0028_rev	CCTGTATCCTCCAGCAAGCTTGTACACATCAACAGGACCTTGACC	Afu2g17600 (*pksP*)
oARK0029_for	TCGCATGCTAAGGCCTGTGGTACCACATCAACAGGACCTTGACC	Afu2g17600 (*pksP*)
oARK0030_rev	TCCGGGGCCCAGGTACCACAGGAAACCTCCTTACTAACCCGG	Afu2g17600 (*pksP*)
oARK0096_for	TGCGCAGTGGCAGCTCTAGAGCTAGCTTTCCTCTTGGAG CAAAAGT	pSilent-pksP2
oARK0038_rev	AAGGAGGTTTAAGCTTGTACGTACCTCGAGTGTGATGTG ATGGAGTTGAG	pSilent-pksP2
oARK0067_for	GAGCTCCACCGCGGTGGCGGCCGCCTTTGCCCGGTGTA TGAAAC	ble, TetON
oARK0068_rev	AGACTAGTTCTAGATACGTATCTAGAAAGAAGGATTACCT	ble, TetON
T7_pabA_500_1_for	TAATACGACTCACTATAGGGAGAATTCCGATAGGACGAT TGCC	Afu6g04820 (pabA)
T7_pabA_500_1_rev	TAATACGACTCACTATAGGGAGAACAAGAAGAAGTGCTG GTGC	Afu6g04820 (pabA)
T7_pabA_500_2_for	TAATACGACTCACTATAGGGAGACAGACTAGATTCTCCG GAAC	Afu6g04820 (pabA)
T7_pabA_500_2_rev	TAATACGACTCACTATAGGGAGACCGAGATAATACTATAC CTC	Afu6g04820 (pabA)
pabA_qRT_for	TACGAACTGTGTCTCACTGG	Afu6g04820 (pabA)
pabA_qRT_rev	TCAGACGTTTGTACAGCTCC	Afu6g04820 (pabA)
coxV_qRT_for	ATCTGTTCGCCAAGCCCAAG	Afu5g10560 (cox5)
coxV_qRT_rev	TCACTGCTGACACCGTAGAG	Afu5g10560 (cox5)

Table S2. Strains and plasmids used in this study.

Strain/Plasmid	Genotype and/or phenotype	Citation
A. fumigatus		
CEA17Δ*akuB*	*akuB*^{KU80}::*pyrG*; PyrG^{+}, Δ*akuB*	(da Silva Ferreira et al. 2006)
Δ*dclA*	CEA17Δ*akuB*, PT^{R}	This study
Δ*dclB*	CEA17Δ*akuB*, Hyg^{R}	This study
Δ*dclA* Δ*dclB*	CEA17Δ*akuB*, PT^{R}, Hyg^{R}	This study
Δ*ppdA*	CEA17Δ*akuB*, Phleo^{R}	This study
Δ*ppdB*	CEA17Δ*akuB*, PT^{R}	This study
Δ*ppdA* Δ*ppdB*	CEA17Δ*akuB*, Phleo^{R}, PT^{R}	This study
Δ*rppA*	CEA17Δ*akuB*, PT^{R}	This study
Δ*rppB*	CEA17Δ*akuB*, Hyg^{R}	This study
Δ*rppA* Δ*rppB*	CEA17Δ*akuB*, PT^{R}, Hyg^{R}	This study
CEA17Δ*akuB_pksP*-IRT	CEA17Δ*akuB*, Hyg^{R}	This study
Δ*dclA_pksP*-IRT	CEA17Δ*akuB*, PT^{R}	This study
ΔdclB_*pksP*-IRT	CEA17Δ*akuB*, Hyg^{R}	This study

Δ*dclA* Δ*dclB_pksP*-IRT	CEA17Δ*akuB*, PT^R, Hyg^R	This study
Δ*ppdA_pksP*-IRT	CEA17Δ*akuB*, Phleo^R	This study
Δ*ppdB_pksP*-IRT	CEA17Δ*akuB*, PT^R	This study
Δ*ppdA* Δ*ppdB_pksP*-IRT	CEA17Δ*akuB*, Phleo^R, PT^R	This study
Δ*rppA_pksP*-IRT	CEA17Δ*akuB*, PT^R	This study
Δ*rppB_pksP*-IRT	CEA17Δ*akuB*, Hyg^R	This study
Δ*rppA* Δ*rppB_pksP*-IRT	CEA17Δ*akuB*, PT^R, Hyg^R	This study
CEA17Δ*akuB_pabA*-IRT	CEA17Δ*akuB*, Phleo^R	This study
E. coli DH5α	*fhuA2, phoA, glnV44, gyrA96, recA1, relA1, endA1, thi-1,* hsdR17, Δ*lacU169,* Φ80' *lacZ*Δ*M*15	MAM department; HKI
AfS150	ATCC46645, pgpdA::dTomato, PT^R	(Lother et al. 2014)
Plasmids		
pSK275	*ptrA*, *oriT*, Amp^R (*bla*)	(Szewczyk and Krappmann 2010)
pJWx16	*hph*, *oriT*, Amp^R (*bla*)	Weber, J., HKI Jena
pJWx46	*ble*, *oriT*, Amp^R (*bla*)	Weber, J., HKI Jena
pSilent1	*hph*, *oriT*, Amp^R (*bla*)	(Nakayashiki et al. 2005)
pSilent-*pksP*1	*hph*, *oriT*, Amp^R (*bla*)	This study
pSilent-*pksP*2	*ble*, *oriT*, Amp^R (*bla*)	This study
pSilent-*pabA*	*ble*, *oriT*, Amp^R (*bla*)	This study

SUPPLEMENTARY DATASETS

Dataset S1. List of the genetic variants identified in RNAi machinery of 300 sequenced *A. fumigatus* isolates first described in (Barber et al. 2021).

Dataset S2. LC-MS/MS proteomics results performed on 48-hour-old mycelia of wild-type and RNAi double knockout strains.

Dataset S3. Gene ontology categories of upregulated and downregulated proteins described in **Dataset 2**.

REFERENCES

Abdel-Hadi AM, Caley DP, Carter DR, Magan N. 2011. Control of aflatoxin production of *Aspergillus flavus* and *Aspergillus parasiticus* using RNA silencing technology by targeting *aflD* (*nor-1*) gene. *Toxins (Basel)* **3**: 647-659.

Agrawal N, Dasaradhi PV, Mohmmed A, Malhotra P, Bhatnagar RK, Mukherjee SK. 2003. RNA interference: biology, mechanism, and applications. *Microbiol Mol Biol Rev* **67**: 657-685.

Alexander WG, Raju NB, Xiao H, Hammond TM, Perdue TD, Metzenberg RL, Pukkila PJ, Shiu PK. 2008. DCL-1 colocalizes with other components of the MSUD machinery and is required for silencing. *Fungal Genet Biol* **45**: 719-727.

Araujo D, Azevedo NM, Barbosa A, Almeida C, Rodrigues ME, Henriques M, Silva S. 2019. Application of 2'-OMethylRNA' Antisense Oligomer to Control *Candida albicans* EFG1 Virulence Determinant. *Mol Ther Nucleic Acids* **18**: 508-517.

Ashburner M, Ball CA, Blake JA, Botstein D, Butler H, Cherry JM, Davis AP, Dolinski K, Dwight SS, Eppig JT et al. 2000. Gene ontology: tool for the unification of biology. The Gene Ontology Consortium. *Nat Genet* **25**: 25-29.

Barber AE, Riedel J, Sae-Ong T, Kang K, Brabetz W, Panagiotou G, Deising HB, Kurzai O. 2020. Effects of Agricultural Fungicide Use on *Aspergillus fumigatus* Abundance, Antifungal Susceptibility, and Population Structure. *mBio* **11**.

Barber AE, Sae-Ong T, Kang K, Seelbinder B, Li J, Walther G, Panagiotou G, Kurzai O. 2021. *Aspergillus fumigatus* pan-genome analysis identifies genetic variants associated with human infection. *Nat Microbiol* **6**: 1526-1536.

Beauvais A, Bozza S, Kniemeyer O, Formosa C, Balloy V, Henry C, Roberson RW, Dague E, Chignard M, Brakhage AA et al. 2013. Deletion of the alpha-(1,3)-glucan synthase genes induces a restructuring of the conidial cell wall responsible for the avirulence of *Aspergillus fumigatus*. *PLoS Pathog* **9**: e1003716.

Billmyre RB, Calo S, Feretzaki M, Wang X, Heitman J. 2013. RNAi function, diversity, and loss in the fungal kingdom. *Chromosome Res* **21**: 561-572.

Bostian KA, Hopper JE, Rogers DT, Tipper DJ. 1980. Translational analysis of the killer-associated virus-like particle dsRNA genome of *S. cerevisiae*: M dsRNA encodes toxin. *Cell* **19**: 403-414.

Brakhage AA, K. ZA, Rivieccio F, Visser C, Blango MG. 2021. Host-derived extracellular vesicles for antimicrobial defense. *microLife*.

Brennan P. 2018. drawProteins: a Bioconductor/R package for reproducible and programmatic generation of protein schematics. *F1000Res* **7**: 1105.

Brown JS, Aufauvre-Brown A, Brown J, Jennings JM, Arst H, Jr., Holden DW. 2000. Signature-tagged and directed mutagenesis identify PABA synthetase as essential for *Aspergillus fumigatus* pathogenicity. *Mol Microbiol* **36**: 1371-1380.

Bruch A, Kelani AA, Blango MG. 2021. RNA-based therapeutics to treat human fungal infections. *Trends Microbiol*.

Burnett JC, Rossi JJ. 2012. RNA-based therapeutics: current progress and future prospects. *Chem Biol* **19**: 60-71.

Cai Q, He B, Weiberg A, Buck AH, Jin H. 2019. Small RNAs and extracellular vesicles: New mechanisms of cross-species communication and innovative tools for disease control. *PLoS Pathog* **15**: e1008090.

Cai Q, Qiao L, Wang M, He B, Lin FM, Palmquist J, Huang SD, Jin H. 2018. Plants send small RNAs in extracellular vesicles to fungal pathogen to silence virulence genes. *Science* **360**: 1126-1129.

Calo S, Nicolas FE, Lee SC, Vila A, Cervantes M, Torres-Martinez S, Ruiz-Vazquez RM, Cardenas ME, Heitman J. 2017. A non-canonical RNA degradation pathway suppresses RNAi-dependent epimutations in the human fungal pathogen *Mucor circinelloides*. *PLoS Genet* **13**: e1006686.

Carreras-Villasenor N, Esquivel-Naranjo EU, Villalobos-Escobedo JM, Abreu-Goodger C, Herrera-Estrella A. 2013. The RNAi machinery regulates growth and development in the filamentous fungus *Trichoderma atroviride*. *Mol Microbiol* **89**: 96-112.

Chen Y, Gao Q, Huang M, Liu Y, Liu Z, Liu X, Ma Z. 2015. Characterization of RNA silencing components in the plant pathogenic fungus *Fusarium graminearum*. *Sci Rep* **5**: 12500.

Corbett KS, Edwards DK, Leist SR, Abiona OM, Boyoglu-Barnum S, Gillespie RA, Himansu S, Schafer A, Ziwawo CT, DiPiazza AT et al. 2020. SARS-CoV-2 mRNA vaccine design enabled by prototype pathogen preparedness. *Nature* **586**: 567-571.

D'Souza CA, Kronstad JW, Taylor G, Warren R, Yuen M, Hu G, Jung WH, Sham A, Kidd SE, Tangen K et al. 2011. Genome variation in *Cryptococcus gattii*, an emerging pathogen of immunocompetent hosts. *mBio* **2**: e00342-00310.

da Silva Ferreira ME, Kress MR, Savoldi M, Goldman MH, Hartl A, Heinekamp T, Brakhage AA, Goldman GH. 2006. The akuB(KU80) mutant deficient for nonhomologous end joining is a powerful tool for analyzing pathogenicity in *Aspergillus fumigatus*. *Eukaryot Cell* **5**: 207-211.

Dang Y, Yang Q, Xue Z, Liu Y. 2011. RNA interference in fungi: pathways, functions, and applications. *Eukaryot Cell* **10**: 1148-1155.

Ender C, Meister G. 2010. Argonaute proteins at a glance. *J Cell Sci* **123**: 1819-1823.

Fedorova O, Jagdmann GE, Jr., Adams RL, Yuan L, Van Zandt MC, Pyle AM. 2018. Small molecules that target group II introns are potent antifungal agents. *Nat Chem Biol* **14**: 1073-1078.

Feretzaki M, Billmyre RB, Clancey SA, Wang X, Heitman J. 2016. Gene Network Polymorphism Illuminates Loss and Retention of Novel RNAi Silencing Components in the *Cryptococcus* Pathogenic Species Complex. *PLoS Genet* **12**: e1005868.

Fisher MC, Gurr SJ, Cuomo CA, Blehert DS, Jin H, Stukenbrock EH, Stajich JE, Kahmann R, Boone C, Denning DW et al. 2020. Threats Posed by the Fungal Kingdom to Humans, Wildlife, and Agriculture. *mBio* **11**.

Gene Ontology C. 2021. The Gene Ontology resource: enriching a GOld mine. *Nucleic Acids Res* **49**: D325-D334.

Gibbons JG, D'Avino P, Zhao S, Cox GW, Rinker DC, Fortwendel JR, Latge J-P. 2022. Comparative Genomics Reveals a Single Nucleotide Deletion in *pksP* That Results in White-Spore Phenotype in Natural Variants of *Aspergillus fumigatus*. *Frontiers in Fungal Biology* **3**.

Gusa A, Williams JD, Cho JE, Averette AF, Sun S, Shouse EM, Heitman J, Alspaugh JA, Jinks-Robertson S. 2020. Transposon mobilization in the human fungal pathogen *Cryptococcus* is mutagenic during infection and promotes drug resistance in vitro. *Proc Natl Acad Sci U S A* **117**: 9973-9980.

Hammond TM, Andrewski MD, Roossinck MJ, Keller NP. 2008a. *Aspergillus* mycoviruses are targets and suppressors of RNA silencing. *Eukaryot Cell* **7**: 350-357.

Hammond TM, Bok JW, Andrewski MD, Reyes-Dominguez Y, Scazzocchio C, Keller NP. 2008b. RNA silencing gene truncation in the filamentous fungus *Aspergillus nidulans*. *Eukaryot Cell* **7**: 339-349.

Hammond TM, Keller NP. 2005. RNA silencing in *Aspergillus nidulans* is independent of RNA-dependent RNA polymerases. *Genetics* **169**: 607-617.

Hou Y, Zhai Y, Feng L, Karimi HZ, Rutter BD, Zeng L, Choi DS, Zhang B, Gu W, Chen X et al. 2019. A Phytophthora Effector Suppresses Trans-Kingdom RNAi to Promote Disease Susceptibility. *Cell Host Microbe* **25**: 153-165 e155.

Hutvagner G, Simard MJ. 2008. Argonaute proteins: key players in RNA silencing. *Nat Rev Mol Cell Biol* **9**: 22-32.

Janbon G, Maeng S, Yang DH, Ko YJ, Jung KW, Moyrand F, Floyd A, Heitman J, Bahn YS. 2010. Characterizing the role of RNA silencing components in *Cryptococcus neoformans*. *Fungal Genet Biol* **47**: 1070-1080.

Jinek M, Doudna JA. 2009. A three-dimensional view of the molecular machinery of RNA interference. *Nature* **457**: 405-412.

Jochl C, Loh E, Ploner A, Haas H, Huttenhofer A. 2009. Development-dependent scavenging of nucleic acids in the filamentous fungus *Aspergillus fumigatus*. *RNA Biol* **6**: 179-186.

Kadotani N, Nakayashiki H, Tosa Y, Mayama S. 2003. RNA silencing in the phytopathogenic fungus *Magnaporthe oryzae*. *Mol Plant Microbe Interact* **16**: 769-776.

Kalleda N, Naorem A, Manchikatla RV. 2013. Targeting fungal genes by diced siRNAs: a rapid tool to decipher gene function in *Aspergillus nidulans*. *PLoS One* **8**: e75443.

Kanhayuwa L, Kotta-Loizou I, Ozkan S, Gunning AP, Coutts RH. 2015. A novel mycovirus from *Aspergillus fumigatus* contains four unique dsRNAs as its genome and is infectious as dsRNA. *Proc Natl Acad Sci U S A* **112**: 9100-9105.

Ketting RF. 2011. The many faces of RNAi. *Dev Cell* **20**: 148-161.

Khatri M, Rajam MV. 2007. Targeting polyamines of *Aspergillus nidulans* by siRNA specific to fungal ornithine decarboxylase gene. *Med Mycol* **45**: 211-220.

Koch A, Hofle L, Werner BT, Imani J, Schmidt A, Jelonek L, Kogel KH. 2019. SIGS vs HIGS: a study on the efficacy of two dsRNA delivery strategies to silence *Fusarium* FgCYP51 genes in infected host and non-host plants. *Mol Plant Pathol* **20**: 1636-1644.

Langfelder K, Jahn B, Gehringer H, Schmidt A, Wanner G, Brakhage AA. 1998. Identification of a polyketide synthase gene (*pksP*) of *Aspergillus fumigatus* involved in conidial pigment biosynthesis and virulence. *Med Microbiol Immunol* **187**: 79-89.

Latge JP. 1999. *Aspergillus fumigatus* and aspergillosis. *Clin Microbiol Rev* **12**: 310-350.

Latge JP, Chamilos G. 2019. *Aspergillus fumigatus* and Aspergillosis in 2019. *Clin Microbiol Rev* **33**.

Lee HC, Li L, Gu W, Xue Z, Crosthwaite SK, Pertsemlidis A, Lewis ZA, Freitag M, Selker EU, Mello CC et al. 2010. Diverse pathways generate microRNA-like RNAs and Dicer-independent small interfering RNAs in fungi. *Mol Cell* **38**: 803-814.

Lother J, Breitschopf T, Krappmann S, Morton CO, Bouzani M, Kurzai O, Gunzer M, Hasenberg M, Einsele H, Loeffler J. 2014. Human dendritic cell subsets display distinct interactions with the pathogenic mould *Aspergillus fumigatus*. *Int J Med Microbiol* **304**: 1160-1168.

Moazed D. 2009. Small RNAs in transcriptional gene silencing and genome defence. *Nature* **457**: 413-420.

Mousavi B, Hedayati MT, Teimoori-Toolabi L, Guillot J, Alizadeh A, Badali H. 2015. cyp51A gene silencing using RNA interference in azole-resistant *Aspergillus fumigatus*. *Mycoses* **58**: 699-706.

Mouyna I, Henry C, Doering TL, Latge JP. 2004. Gene silencing with RNA interference in the human pathogenic fungus *Aspergillus fumigatus*. *FEMS Microbiol Lett* **237**: 317-324.

Mukherjee K, Campos H, Kolaczkowski B. 2013. Evolution of animal and plant dicers: early parallel duplications and recurrent adaptation of antiviral RNA binding in plants. *Mol Biol Evol* **30**: 627-641.

Murata T, Kadotani N, Yamaguchi M, Tosa Y, Mayama S, Nakayashiki H. 2007. siRNA-dependent and -independent post-transcriptional cosuppression of the LTR-retrotransposon MAGGY in the phytopathogenic fungus *Magnaporthe oryzae*. *Nucleic Acids Res* **35**: 5987-5994.

Nakayashiki H, Hanada S, Nguyen BQ, Kadotani N, Tosa Y, Mayama S. 2005. RNA silencing as a tool for exploring gene function in ascomycete fungi. *Fungal Genet Biol* **42**: 275-283.

Nami S, Baradaran B, Mansoori B, Kordbacheh P, Rezaie S, Falahati M, Mohamed Khosroshahi L, Safara M, Zaini F. 2017. The Utilization of RNA Silencing Technology to Mitigate the Voriconazole Resistance of *Aspergillus Flavus*; Lipofectamine-Based Delivery. *Adv Pharm Bull* **7**: 53-59.

Nicolas FE, Garre V. 2016. RNA Interference in Fungi: Retention and Loss. *Microbiol Spectr* **4**.

Nicolas FE, Moxon S, de Haro JP, Calo S, Grigoriev IV, Torres-Martinez S, Moulton V, Ruiz-Vazquez RM, Dalmay T. 2010. Endogenous short RNAs generated by Dicer 2 and RNA-dependent RNA polymerase 1 regulate mRNAs in the basal fungus *Mucor circinelloides*. *Nucleic Acids Res* **38**: 5535-5541.

Nicolas FE, Vila A, Moxon S, Cascales MD, Torres-Martinez S, Ruiz-Vazquez RM, Garre V. 2015. The RNAi machinery controls distinct responses to environmental signals in the basal fungus *Mucor circinelloides*. *BMC Genomics* **16**: 237.

Nuss DL. 2011. Mycoviruses, RNA silencing, and viral RNA recombination. *Adv Virus Res* **80**: 25-48.

Oberegger H, Zadra I, Schoeser M, Haas H. 2000. Iron starvation leads to increased expression of Cu/Zn-superoxide dismutase in *Aspergillus*. *FEBS Lett* **485**: 113-116.

Ozkan S, Mohorianu I, Xu P, Dalmay T, Coutts RHA. 2017. Profile and functional analysis of small RNAs derived from Aspergillus fumigatus infected with double-stranded RNA mycoviruses. *BMC Genomics* **18**: 416.

Perez-Riverol Y, Bai J, Bandla C, Garcia-Seisdedos D, Hewapathirana S, Kamatchinathan S, Kundu DJ, Prakash A, Frericks-Zipper A, Eisenacher M et al. 2022. The PRIDE database resources in 2022: a hub for mass spectrometry-based proteomics evidences. *Nucleic Acids Res* **50**: D543-D552.

Qin H, Chen F, Huan X, Machida S, Song J, Yuan YA. 2010. Structure of the *Arabidopsis thaliana* DCL4 DUF283 domain reveals a noncanonical double-stranded RNA-binding fold for protein-protein interaction. *RNA* **16**: 474-481.

Romano N, Macino G. 1992. Quelling: transient inactivation of gene expression in *Neurospora crassa* by transformation with homologous sequences. *Mol Microbiol* **6**: 3343-3353.

Ruiz-Vazquez RM, Nicolas FE, Torres-Martinez S, Garre V. 2015. Distinct RNAi Pathways in the Regulation of Physiology and Development in the Fungus *Mucor circinelloides*. *Adv Genet* **91**: 55-102.

Schauer SE, Jacobsen SE, Meinke DW, Ray A. 2002. DICER-LIKE1: blind men and elephants in *Arabidopsis* development. *Trends Plant Sci* **7**: 487-491.

Shabalina SA, Koonin EV. 2008. Origins and evolution of eukaryotic RNA interference. *Trends Ecol Evol* **23**: 578-587.

Shopova IA, Belyaev I, Dasari P, Jahreis S, Stroe MC, Cseresnyes Z, Zimmermann AK, Medyukhina A, Svensson CM, Kruger T et al. 2020. Human Neutrophils Produce Antifungal Extracellular Vesicles against *Aspergillus fumigatus*. *mBio* **11**.

Song MS, Rossi JJ. 2017. Molecular mechanisms of Dicer: endonuclease and enzymatic activity. *Biochem J* **474**: 1603-1618.

Southern E. 2006. Southern blotting. *Nat Protoc* **1**: 518-525.

Szewczyk E, Krappmann S. 2010. Conserved regulators of mating are essential for *Aspergillus fumigatus* cleistothecium formation. *Eukaryot Cell* **9**: 774-783.

Torres-Martinez S, Ruiz-Vazquez RM. 2017. The RNAi Universe in Fungi: A Varied Landscape of Small RNAs and Biological Functions. *Annu Rev Microbiol* **71**: 371-391.

Wang X, Wang P, Sun S, Darwiche S, Idnurm A, Heitman J. 2012. Transgene induced co-suppression during vegetative growth in *Cryptococcus neoformans*. *PLoS Genet* **8**: e1002885.

Weiberg A, Wang M, Lin FM, Zhao H, Zhang Z, Kaloshian I, Huang HD, Jin H. 2013. Fungal small RNAs suppress plant immunity by hijacking host RNA interference pathways. *Science* **342**: 118-123.

Weidner G, d'Enfert C, Koch A, Mol PC, Brakhage AA. 1998. Development of a homologous transformation system for the human pathogenic fungus *Aspergillus fumigatus* based on the pyrG gene encoding orotidine 5'-monophosphate decarboxylase. *Curr Genet* **33**: 378-385.

Wessel D, Flugge UI. 1984. A method for the quantitative recovery of protein in dilute solution in the presence of detergents and lipids. *Anal Biochem* **138**: 141-143.

Witwer KW, Wolfram J. 2021. Extracellular vesicles versus synthetic nanoparticles for drug delivery. *Nature Reviews Materials*.

A

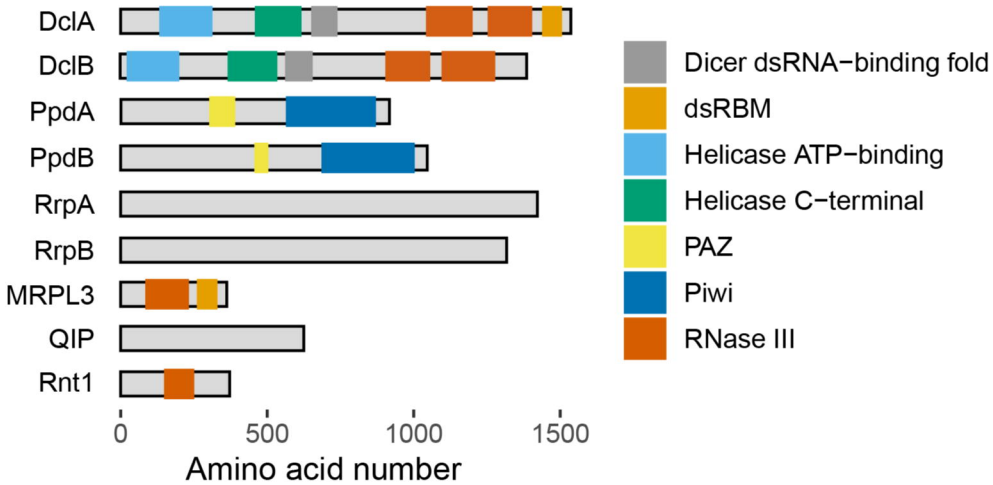
DclA
DclB
PpdA
PpdB
RrpA
RrpB
MRPL3
QIP
Rnt1
0
500
1000
1500
Amino acid number
Dicer dsRNA−binding fold
dsRBM
Helicase ATP−binding
Helicase C−terminal
PAZ
Piwi
RNase III

B

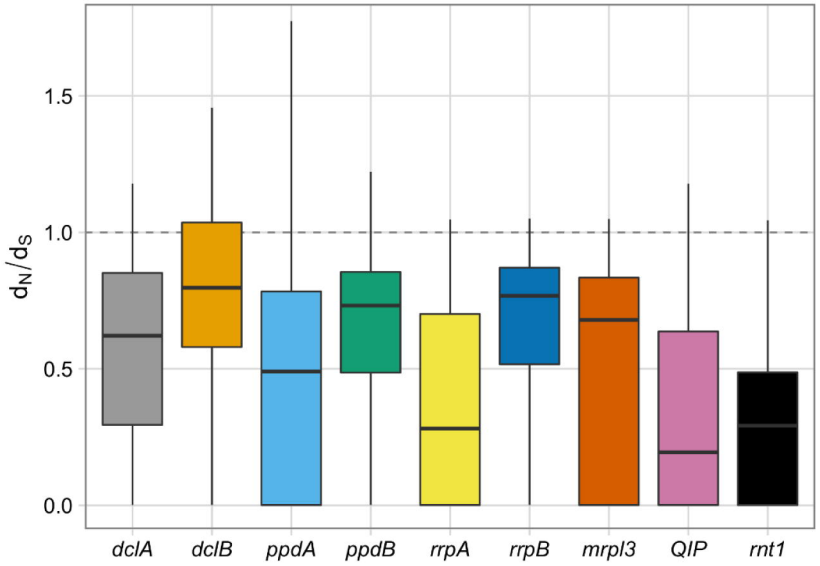
1.5
1.0
0.5
0.0
d_N/d_S
dclA
dclB
ppdA
ppdB
rrpA
rrpB
mrpl3
QIP
rnt1

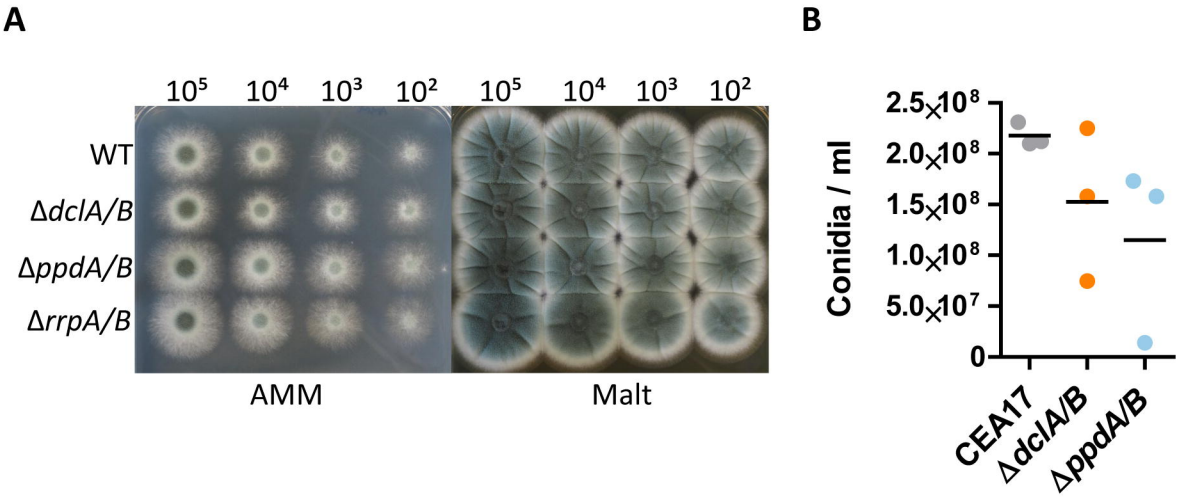
A
B
10⁵
10⁴
10³
10²
WT
ΔdclA/B
ΔppdA/B
ΔrrpA/B
AMM
Malt
Conidia / ml
2.5x10⁸
2.0x10⁸
1.5x10⁸
1.0x10⁸
5.0x10⁷
0
CEA17
ΔdclA/B
ΔppdA/B

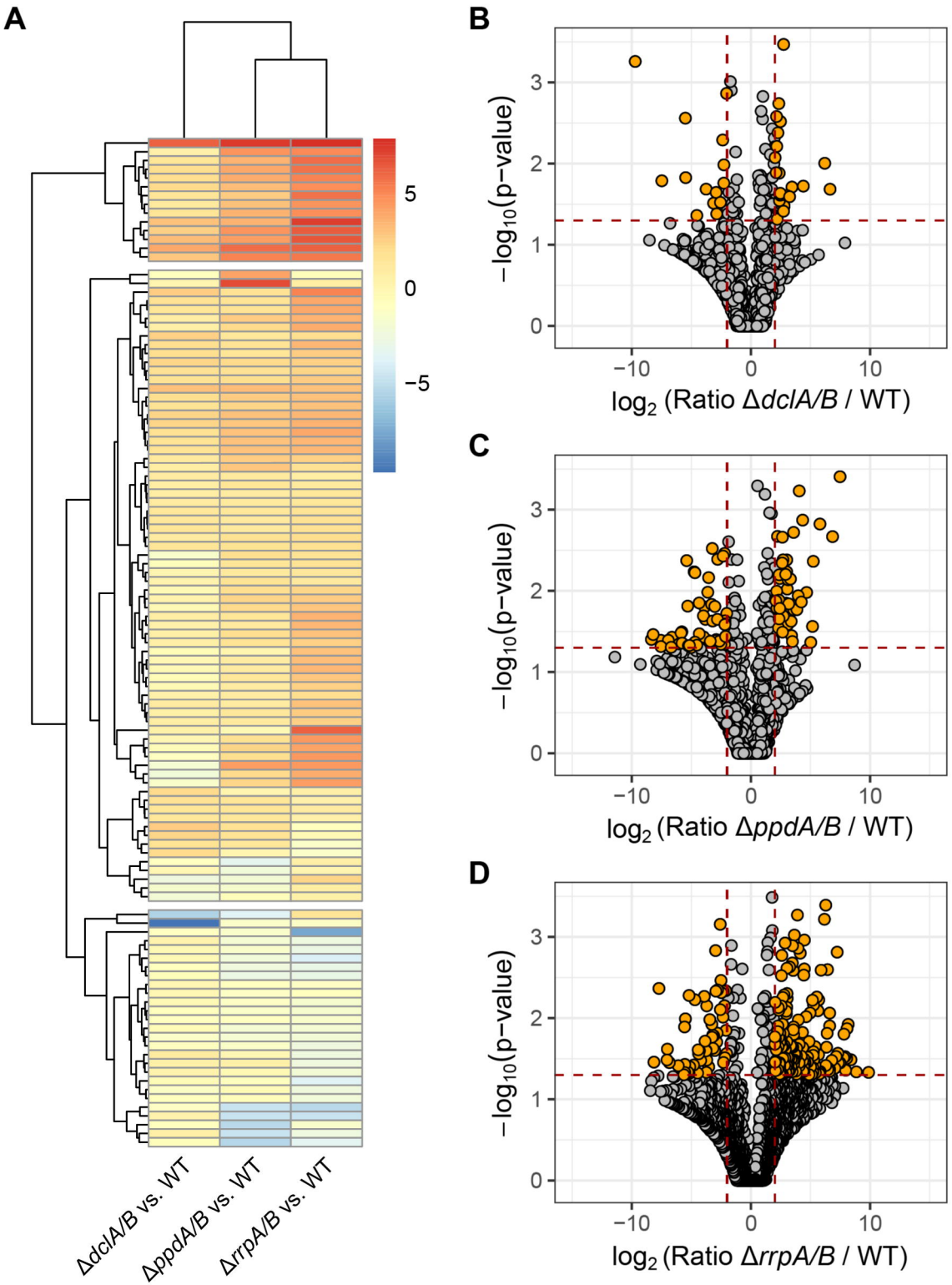
A
5
0
−5
ΔdclA/B vs. WT
ΔppdA/B vs. WT
ΔrrpA/B vs. WT
B
−log10(p−value)
log2 (Ratio ΔdclA/B / WT)
C
−log10(p−value)
log2 (Ratio ΔppdA/B / WT)
D
−log10(p−value)
log2 (Ratio ΔrrpA/B / WT)

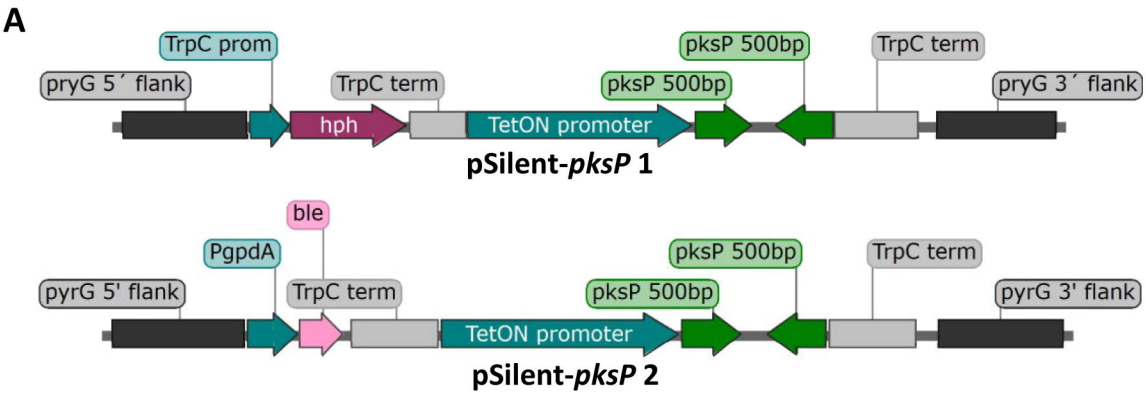
A
TrpC prom
pksP 500bp
TrpC term
pryG 5´ flank
TrpC term
pksP 500bp
pryG 3´ flank
hph
TetON promoter
pSilent-pksP 1
ble
PgpdA
pksP 500bp
TrpC term
pyrG 5' flank
TrpC term
pksP 500bp
pyrG 3' flank
TetON promoter
pSilent-pksP 2

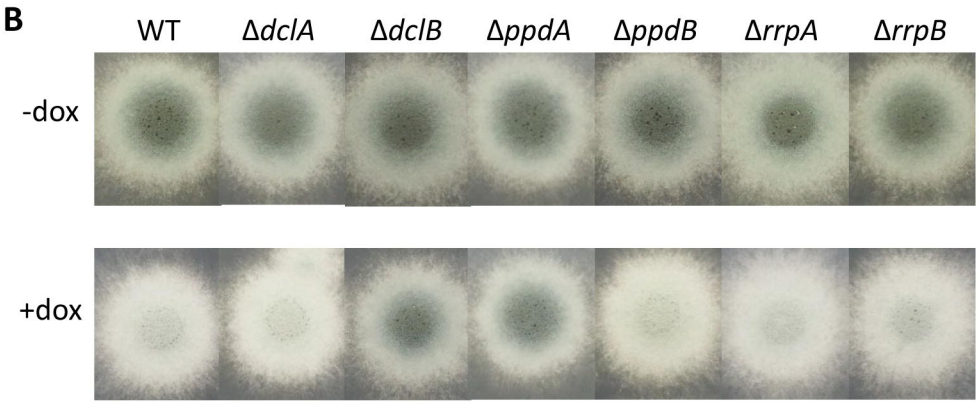
B
WT
ΔdclA
ΔdclB
ΔppdA
ΔppdB
ΔrrpA
ΔrrpB
-dox
+dox

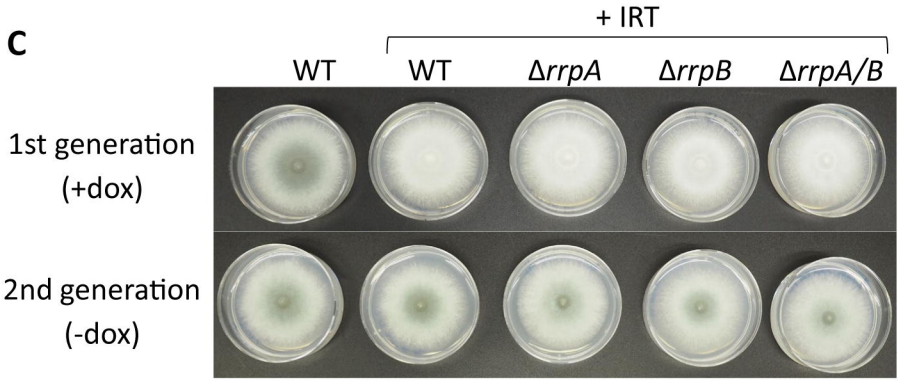
C
+ IRT
WT
WT
ΔrrpA
ΔrrpB
ΔrrpA/B
1st generation
(+dox)
2nd generation
(-dox)

A

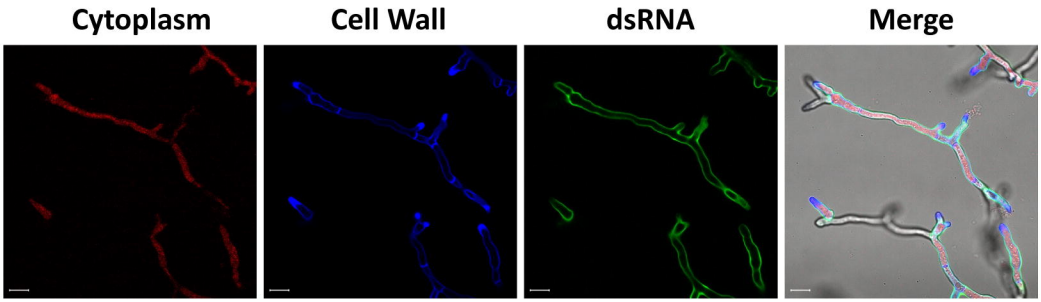
Cytoplasm
Cell Wall
dsRNA
Merge

B

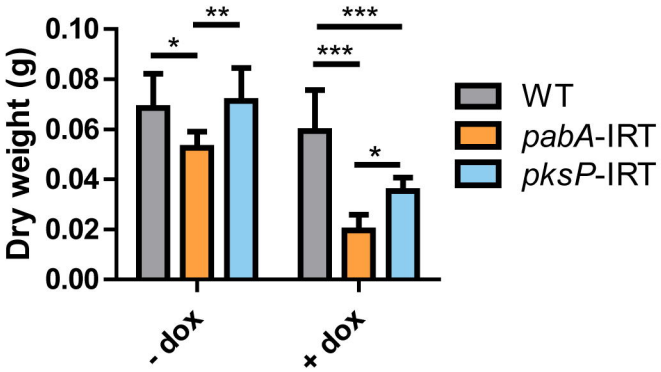
Dry weight (g)
0.10
0.08
0.06
0.04
0.02
0.00
*
**
***
***
*
- dox
+ dox
WT
pabA-IRT
pksP-IRT

C

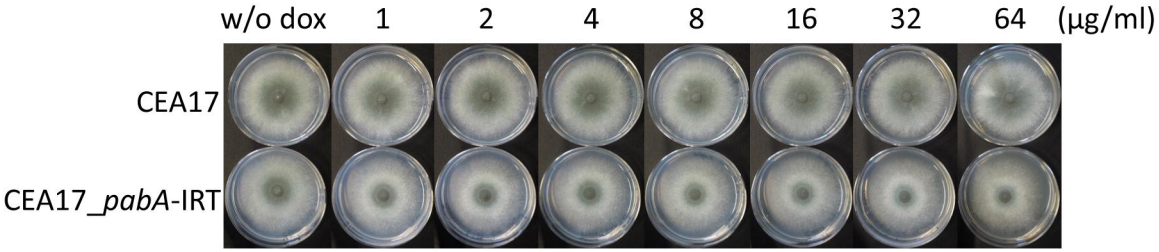
w/o dox
1
2
4
8
16
32
64
(μg/ml)
CEA17
CEA17_pabA-IRT